ELEVENTH EUROPEAN ROTORCRAFT FORUM

Paper No. 77

OPTIMAL CONTROL OF HELICOPTER AEROMECHANICAL STABILITY

F.K. Straub
McDonnell Douglas Helicopter Company
Culver City, California 90230, U.S.A.

September 10-13, 1985

London, England.

THE CITY UNIVERSITY, LONDON, EC1V OHB, ENGLAND.

OPTIMAL CONTROL OF HELICOPTER AEROMECHANICAL STABILITY

F.K. Straub
McDonnell Douglas Helicopter Company
Culver City, California 90230, U.S.A.

ABSTRACT

Optimal control theory is applied to the design of a control system for the elimination of helicopter rotor/body aeromechanical instabilities. Control is introduced through actuators in the fixed system which drive the nonrotating swashplate. The entire range of rotor operating speeds is considered. For the particular configuration studied here, this includes coalescence of the regressing lag mode with the longitudinal and lateral support modes. The optimal controller for the case of reduced blade lead-lag damping is successful in stabilizing the system at all rotor speeds. Furthermore, through successive reduction in the number of measurements, it is shown that feedback of body degrees of freedom alone provides adequate damping augmentation to eliminate the need for lead-lag dampers. This is possible without gain scheduling. The resulting controller is shown to be relatively insensitive with respect to changes in rotor/body parameters.

Notation

A	=	System dynamics matrix
B	=	Control distribution matrix
c_ζ	=	Lag damper constant
C_x, C_y	=	Fuselage damping constants
C_l	=	Output scaling matrix
e	=	Blade root hinge offset
h	=	Offset of rotor hub from fuselage c.g.
k	=	Blade index, k=1, ... N
K_l	=	Feedback gain matrix
J	=	Quadratic cost function
M_x, M_y	=	Fuselage effective masses
NR	=	Nominal rotor speed

Q_l = Weighting matrix for outputs

R_x, R_y = Fuselage longitudinal, lateral motion (on some figures x,y is used)

R_l = Weighting matrix for controls

u = Vector of control inputs

x = Vector of state space variables

y = Vector of outputs

β, ζ = Blade flap, lag motion

β_c, β_s = Rotor cosine, sine cyclic flap degrees of freedom

β_p = Precone

ζ_c, ζ_s = Rotor cosine, sine cyclic lead-lag degrees of freedom

θ_o = Rotor collective pitch angle

θ_A = Active control blade feathering angle

θ_{AC}, θ_{AS} = Active control feathering inputs to nonrotating swashplate

θ_G = Blade aerodynamic pitch angle

θ_S = Orientation of blade root springs at flat pitch

θ_x, θ_y = Fuselage roll, pitch motion

σ = Real part of eigenvalue, i.e., modal damping, rad/sec

ϕ = Feedback phase

ψ = Nondimensional time parameter, rotor azimuth

ω = Imaginary part of eigenvalue, i.e., modal frequency, rad/sec

Ω = Rotor speed

$( )_o$ = Steady-state equilibrium value

$(\dot{})$ $d( )/d_\psi$

1. Introduction

Helicopter aeromechanical instability is a continuous challenge for the rotor dynamicist. Generally, considerable design, analysis, and testing effort is spent until an acceptable solution for all operating conditions is found. In many cases it is necessary to use mechanical lead-lag dampers for articulated rotors, or add damping material to increase the blade structural damping for hingeless and bearingless rotors. This can result in

increased cost, complexity, maintenance, weight, and hub drag. In addition, soft inplane hingeless rotor configurations without damping augmentation have inherently low rotor blade structural damping. These systems have not been used extensively in the helicopter industry, in part, because of poor aeroelastic stability characteristics. Consequently a means to increase aeromechanical stability in a reliable manner could significantly improve the operational characteristics of this rotor hub design.

The use of active blade pitch control has been successfully demonstrated for vibration reduction (Ref. 1). A significant amount of analytical and experimental research has been performed to develop this technology for both N per rev and gust-induced vibration control. The technology is now available for advanced applications.

In a previous study (Ref. 2) the concept of active control blade feathering to augment rotor/fuselage damping was explored. It was shown that feedback of a single state variable with the appropriate feedback gain and phase can increase damping levels considerably and eliminate ground resonance instabilities for a wide variety of rotor configurations. The present study extends these results by employing multivariable optimal control theory techniques.

The purpose of the present study is to show that a feedback control system with a small number of feedback loops and limited scheduling of gains can be used to control aeromechanical stability at all rotor speeds. Feedback gains could then be precomputed off-line, resulting in a simple and low cost controller. On-line system identification would not be necessary. The detailed objectives of the present study are:

(1) Apply multivariable optimal control theory to study the effects of full state feedback on system damping. Results from this controller will serve as baseline against which the performance of simpler controllers will be evaluated.

(2) Investigate the effectiveness of simplified controllers through systematic reduction of the number of measurements and feedback loops.

(3) Assess the sensitivity of the simple controller with respect to changes in the rotor/body configuration parameters.

The analytical rotor/body model used for numerical simulations is briefly discussed in the next section. This is followed by a description of the control design process. Finally, active control results for the aeromechanical stability of a full size rotor on a wind tunnel support stand are presented to show the potential of the proposed approach.

2. Analytical Model

The mathematical rotor/fuselage model employed in the present study is the same as the one used in Ref. 2. The essential features of this model are described below.

The helicopter body is represented as a rigid fuselage having pitch and roll rotations (θ_y,θ_x) about the center of mass and longitudinal and lateral translations (R_x,R_y) of the center of mass, see Fig. 1. The

fuselage physical properties required for modeling are its mass, pitch and roll inertias, and effective landing gear stiffnesses and damping in rotation and translation. The rotor hub, having three or more blades, is located a distance h directly above the fuselage mass center. The blades are assumed to be rigid and rotate against spring and damper restraints about coincident flap and lead-lag hinges offset from the axis of rotation, see Fig. 2. The orientation of the hinges can be different from the aerodynamic pitch angle, thus allowing modeling of variable structural flap-lag coupling with blade feathering inboard or outboard of the hinges. Blade precone is included. This parameter is particularly important in this study since it directly contributes to the inplane Coriolis forces which augment blade lag damping. In deriving the governing equations, rotor rotation speed is assumed constant. The aerodynamic forces are based on two-dimensional quasi-steady theory. Apparent mass, compressibility and stall are neglected. No low frequency unsteady aerodynamic model (dynamic inflow) is used. The pitch control input is composed of two parts: the time-independent collective pitch, identical for all blades; and the time-varying "active" pitch.

In implementing the active control, it is assumed that feedback is applied through a conventional swashplate, i.e., control motions are generated by actuators in the fixed system. The active pitch input to the k^{th} blade can then be expressed as

$$\theta_{Ak} = \theta_{AC(\psi)} \cos\psi_k + \theta_{AS(\psi)} \sin\psi_k \tag{1}$$

where the control inputs θ_{AC} and θ_{AS} are to be determined functions of the nondimensional time parameter ψ.

The derivation of the equations of motion for this model makes use of an appropriate ordering scheme based on the magnitude of blade slopes (typically $0.1 < \varepsilon < 0.2$). Fuselage motions are assumed to be of order $O(\varepsilon^{1.5})$. The active control portion of the blade pitch angle is assumed to be of order $O(\varepsilon^{1.5})$, based on experience with the higher harmonic control inputs of Ref. 1. In applying the ordering scheme it is assumed that terms of order $O(\varepsilon^2)$ are negligible in comparison with unity. In addition, all terms that contain products of the fuselage degrees of freedom are neglected.

The resulting equations of motion are nonlinear with periodic coefficients. They are linearized about a hover trim equilibrium position.

The linearized periodic coefficient perturbation equations are converted into a constant coefficient system using a multiblade or Fourier coordinate transformation. The final set of equations is

$$[M(q_o)]\ddot{q} + [C(q_o)]\dot{q} + [K(q_o)]q + [F(q_o)]u = 0 \tag{2}$$

$$q^T = [\zeta_c, \beta_c, \zeta_s, \beta_s, \theta_x, \theta_y, R_x, R_y] \tag{3}$$

$$u^T = [\theta_{AC}, \theta_{AS}] \tag{4}$$

where q is the vector of system degrees of freedom and u is the vector of control inputs.

Aeromechanical stability in the fixed system is then evaluated by transforming the equations into first order form and performing an eigenvalue analysis.

Examining the governing equations of motion used in this study shows that the active control pitch input appears as aerodynamic forcing expressions in all equations. The values in the blade lag and fuselage translation equations are one order of magnitude smaller than in the flap equations and in the fuselage pitch and roll equations. From these equations it therefore seems that two primary mechanisms exist to stabilize ground resonance. First, the fuselage motion can be controlled through the forces and moments arising from flapping. The second mechanism is lead-lag damping augmentation through Coriolis coupling with blade flap motion. This requires presence of either steady blade coning deflection or built-in precone.

3. Control System Design

The active control approach in this study is based on the deterministic linear optimal regulator problem. Results for this full state feedback controller are used as baseline against which other controllers are evaluated. Simplified controllers are developed through a systematic reduction in the number of feedback loops while using the feedback gain factors obtained for the optimal controller.

Optimal control theory is applied to the linear, constant coefficient differential equations (Eq. 2) written in first order form.

$$\dot{x} = A\,x + B\,u \tag{5}$$

$$y = C_1\,x \tag{6}$$

where x is the vector of state variables, $x^T = [q, \dot{q}]$, u is the vector of controls defined in Eq. 4, and y is the vector of system outputs. The objective is now to find controls u, that is the cyclic control inputs to the swashplate, which will minimize the quadratic cost function.

$$J = \int_0^\infty \left(y^T \cdot Q_1 \cdot y + u^T \cdot R_1 \cdot u \right) dt \tag{7}$$

where the weighting matrices Q_1 and R_1 are assumed to be symmetric and positive definite. The solution is the deterministic optimal controller (Ref. 3) with linear feedback of all state variables.

$$u = K_1 x \tag{8}$$

where

$$K_1 = -R_1^{-1} B^T S \tag{9}$$

and the matrix S is the constant, symmetric, positive definite solution of the algebraic Ricatti equation.

$$-S \cdot A - A^T \cdot S + S \cdot B \cdot R_1^{-1} \cdot B^T \cdot S - C_1^T \cdot Q_1 \cdot C_1 = 0 \tag{10}$$

The Ricatti equation is solved by an improved version of Potter's method (Ref. 4). The closed loop dynamics equation is then defined as

$$\dot{x} = \left(A + B \cdot K_1 \right) x \tag{11}$$

In the present study the output scaling matrix C_1 is chosen such that the output vector y corresponds directly to the system displacement degrees of freedom, i.e., system velocity states are not included in the cost function. The weighting matrixes Q_1 and R_1 are assumed to be diagonal. For all results in the paper, unit values were chosen for the weight factors. Other relative values were explored, however it was found that unit values seemed to be a good choice in terms of balancing control effort, system stability, and system response.

Several simplified controllers are derived from the optimal controller through a systematic reduction in the number of feedback loops resulting in a corresponding reduction in the number of required measurements. Particular emphasis is placed on eliminating feedback of rotor degrees of freedom. The gain constants for these reduced state feedback controllers are chosen as the values obtained for the corresponding states in the optimal controller.

The performance of the various controllers is evaluated by examining the open- and closed-loop system dynamic stability throughout the range of rotor operating speeds. In addition, the sensitivity of a candidate, constant gain controller with respect to uncertainties or changes in rotor/body configuration parameters is evaluated.

4. Results and Discussion

4.1 Baseline System

All numerical simulations in this study were performed for a full-size H-34 rotor mounted on the Rotor Test Apparatus (RTA) support structure in the NASA Ames 40 x 80 foot wind tunnel (Fig. 3). The H-34 rotor is 4-bladed and fully articulated, with a hinge offset of 4 percent. It has viscous lead-lag dampers. In addition, the rotor is equipped with a multicyclic control system. The RTA system is supported by three struts. The particular configuration considered here uses 15 foot long struts and the tunnel balance dampers and snubbers are not engaged. This support structure is unique inasmuch as it allows basically only hub longitudinal and lateral translational motions in the frequency range of interest. In the present

study the H-34/RTA system is modeled with two lag, two flap, and two support degrees of freedom, and thus is described by 12 state variables. The basic system properties are given in Table I.

The basic system dynamics, i.e., without active controls, are presented first. Figure 4 shows modal damping and frequencies for the case of nominal blade lead-lag damping and zero collective pitch. The regressing lag mode coalesces with both the support longitudinal and lateral modes, at approximately 140 and 180 rpm, respectively. System stability, governed by the support modes, drops at the coalescence rotor speeds. However, sufficient stability margins exist.

In order to perform meaningful control simulation studies the blade lag damper value is reduced to 10 percent of its nominal value. This essentially represents a case without lead-lag dampers. In addition, blade collective pitch angle had to be introduced in order to make the system controllable. Figure 5 shows the effect of collective pitch on regressing lag mode damping, at the coalescence rotor speeds of 140 and 180 rpm. Note, that at flat pitch the system with reduced lag damping is unstable at both these rotor speeds. Increasing blade collective adds damping to the system, until at 10 degrees the lag mode is stable at both rotor speeds. A value of 8 degrees collective is chosen for all subsequent studies. This is the value set when running up the H-34/RTA system. Modal damping and frequencies for this system are shown in Fig. 6. System stability is governed by the regressing lag mode damping. At the crossover with the longitudinal mode (140 rpm) the system is marginally stable. At the crossover with the lateral mode the system is unstable. All subsequent active control studies are performed for the system depicted in Fig. 6.

4.2 Controller Development

A summary of the controllers considered in this study and their effectiveness in augmenting rotor/body damping at the critical rotor speeds is shown in Table II. As discussed previously, damping values for the system without controls show marginal stability at 140 rpm and instability at 180 rpm. Controller A, the optimal controller with full state feedback (LQG), is seen to add considerable amount of damping to the system. Controllers B, C, and D are derived from the optimal controller through successive reduction in the number of feedback loops and required measurements. The gain values used are those computed for the optimal controller at the respective rotor speeds. Eliminating flapping from the controller, case B, adds more damping to the system at the two critical rotor speeds than even the optimal controller. However, it was found that at other rotor speeds Controller B actually destabilized the system. It is therefore not further considered here. For Controller C lead-lag is also eliminated from the feedback. It is seen that working with fixed system measurements alone is entirely sufficient to stabilize the system. Lastly, Controller D requires only measurement of the longitudinal and lateral rates and is still able to augment damping even though to a lesser degree.

The controller performance in improving system stability at all rotor speeds is investigated next. Figure 7 shows the damping of five different systems versus rotor speed. The solid line (u=0) indicates stability of the system with reduced blade lag damping and zero control. It is seen that the system without lag dampers is marginally stable at 140 rpm and

unstable at 180 rpm. Next, using optimal control theory a gain scheduled controller with full state feedback is applied (LQG). The optimal control problem is solved at several rotor speeds in increments of 10 rpm. The figure shows that with this controller system damping is improved to the point where the system without lag dampers, for rotor speeds between 120 and 210 rpm, is even more stable than the baseline system with nominal blade damping and zero controls (u=0, c_ζ=3200 Nms). While the LQG controller works extremely well it requires 12 measurements and storage of 24 gain constants at each rpm value in the control schedule.

A reduced state feedback controller with fixed gains is designed for the system without lag dampers. This controller represents an ad hoc approach based on the physical insight gained from previous studies (Ref. 2). The LQG gains for the longitudinal displacement and rate at 140 rpm and the lateral displacement and rate at 180 rpm are used in feedback of those four system states. Feedback of rotor states is eliminated all together. Results in Fig. 7 show that this simple controller with only four gain constants, $u=u(x,y,\dot{x},\dot{y})$, and without any gain scheduling yields a stable system at all rotor speeds. Between approximately 130 and 200 rpm this controller augments system damping to the levels present in the system with nominal lag dampers. A further simplification is made by eliminating longitudinal and lateral displacement feedback loops. The resulting controller requiring only two measurements is also successful in stabilizing the system although to a lesser degree. However, damping exhibits the typical drop at the coalescence rotor speeds. In summary, it is felt that the controller with four feedback loops represents a good compromise in terms of damping augmentation and controller complexity. All following results are based on this simple controller and the optimal controller.

Figure 8 shows the effect of the simple controller on modal frequencies. It is seen that only small changes occur at the coalescence rotor speeds and that frequencies are not changed at other rotor speeds. This clearly indicates that improvements in system stability as a result of active control are strictly due to increased regressing lead-lag mode damping. System frequencies, and in particular the coalescence rotor speeds, remain essentially unchanged.

The system response after a small lateral rate perturbation is studied next. Figure 9A shows that without any active control the system is quite unstable. Lead-lag amplitudes build up to over two degrees after only ten rotor revolutions. This corresponds to 3.3 seconds at the rotor speed of 180 rpm. With the optimal full state feedback controller, Fig. 9B, the response in any of the system degrees of freedom never exceeds 0.3 degrees. This is accomplished with a maximum active control blade feathering angle of only one third degree. The reduced state feedback controller, Fig. 9C, performs acceptably. After ten rotor revolutions the lead-lag amplitudes have declined to approximately 0.5 degree. The maximum active control blade pitch is about 0.9 degree. The lead-lag amplitudes for the system with nominal lag damping and zero controls decline to approximately 0.6 degree after ten rotor revolutions (results not shown).

Results presented so far show that the controller with feedback of the four support states and constant gains adds considerable damping to the rotor/body system. The sensitivity of this particular control system implementation to changes in support system dynamics and damping is considered next.

4.3 Controller Sensitivity

The sensitivity of the simple, constant gain controller with respect to changes in rotor/body configuration parameters is evaluated. Three modified dynamic systems are considered. The support effective masses, M_x and M_y, are set at 80 percent and then 120 percent of their nominal values. Also, the support effective damping, C_x and C_y, is reduced to 50 percent of nominal values. In all these cases the simple controller is applied with the same feedback gains used previously for the nominal body configuration. These results are intended to show the controller performance at an off-design point and provide a qualitative measure of its robustness.

Figures 10-12 show stability of the modified rotor/support systems as described above. Damping augmentation for the reduced feedback controller, $u = u(x, y, \dot{x}, \dot{y})$, and the optimal controller (LQG) are compared with the open loop system stability ($u = o$). Note, that the optimal control problem for the modified systems is solved at increments of 10 rpm throughout the range of rotor speeds considered.

For changes in the support masses, Figures 10 and 11, the simple controller performs very well. In both cases considerable damping is added to the system. When the support damping is reduced by 50%, Figure 12, the system is unstable at both 140 and 180 rpm. The simple controller is successful in eliminating both instabilities. In summary, it is seen that the proposed simple controller copes very well with changes in rotor/body configuration parameters.

5. Conclusions

Results of the present study show that multivariable optimal control theory is a powerful tool to design a control system for active blade feathering which can considerably improve the helicopter aeromechanical stability behavior. From stability results for a full scale rotor on a wind tunnel test stand the following conclusions can be drawn:

(1) The deterministic optimal controller with full state feedback and rpm scheduled gains adds considerable damping to the system at all rotor speeds. This includes coalescence of the regressing lag mode with the support longitudinal and lateral modes.

(2) Feedback gains computed from optimal control theory can be used to develop a reduced state feedback system.

(3) Feedback of support longitudinal and lateral degrees of freedom alone is sufficient to eliminate the need for lead-lag dampers. Gain scheduling with rotor speed is not required.

(4) System stability improvements are a direct result of increased regressing lag mode damping since system frequencies, and in particular the coalescence rotor speeds, remain unchanged.

(5) The simple reduced state feedback controller performs well when changing rotor body configuration parameters. In particular the system is stabilized when the support damping is reduced by 50 percent.

REFERENCES

1. Wood, E.R., Powers, R.W., Cline, J.H., and Hammond, C.E., "On Developing and Flight Testing a Higher Harmonic Control System," Journal of the American Helicopter Society, Vol. 30, No. 1, January 1985, pp. 3-20.

2. Straub, F.K. and Warmbrodt, W., "The Use of Active Controls to Augment Rotor/Fuselage Stability," Journal of the American Helicopter Society, Vol. 30, No. 1, January 1985, pp. 13-22.

3. Kwakernak, K. and Sivan, R., "Linear Optimal Control Systems," Wiley-Interscience, New York, 1972.

4. Wei, S.Y., "Application of Linear Quadratic Control in Reduction of Aerodynamic Forces on Aircraft," Ph.D. Thesis, Dept. of Mechanical Engineering, Oregon State University, June 1981.

Table I H-34/RTA Properties

Number of blades	4
Rotor radius, m	8.53
Blade chord, m	0.417
Nominal rotor speed, rpm	212
Hinge offset, m	0.305
Lift curve slope	5.73
Profile drag coefficient	0.0079
Lock number	9.7
Blade mass, kg	110
First mass moment, kg m	294
Flap inertia, kg m^2	1596
Lag damper, N m sec, nominal	3200
reduced	320
Support mass longitudinal, kg	29,980
Support mass lateral, kg	24,350
Longitudinal frequency, Hz	1.77
Lateral frequency, Hz	2.34
Damping longitudinal, N sec/m	38,820
Damping lateral, N sec/m	28,410

Table II Summary of Controllers and Their Effectiveness in Augmenting Rotor Body Damping (C_ζ=320 Nms, θ_o=8°)

	Damping — rad/sec	
	140 rpm	180 rpm
Baseline (u=0)	-0.0515	0.0983
A) Optimal Control (LQG)	-0.5578	-0.4995
Feedback: B) $u(\zeta_c,\zeta_s,R_x,R_y,\dot{\zeta}_c,\dot{\zeta}_s,\dot{R}_x,\dot{R}_y)$	-0.5819	-0.6073
C) $u(R_x,R_y,\dot{R}_x,\dot{R}_y)$	-0.4017	-0.3526
D) $u(\dot{R}_x,\dot{R}_y)$	-0.2150	-0.1517

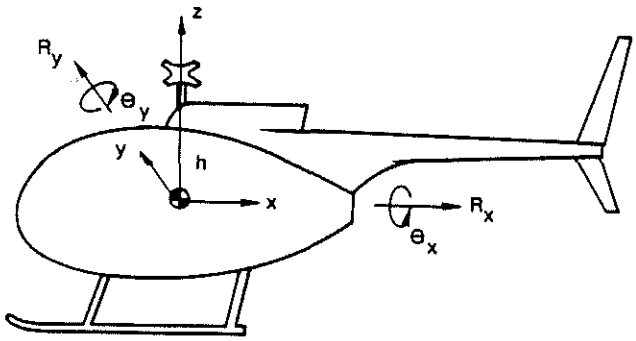

Figure 1. Fuselage Model

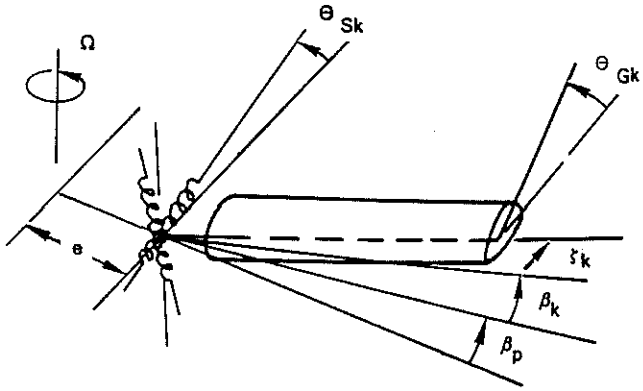

Figure 2. Rotor Blade Model

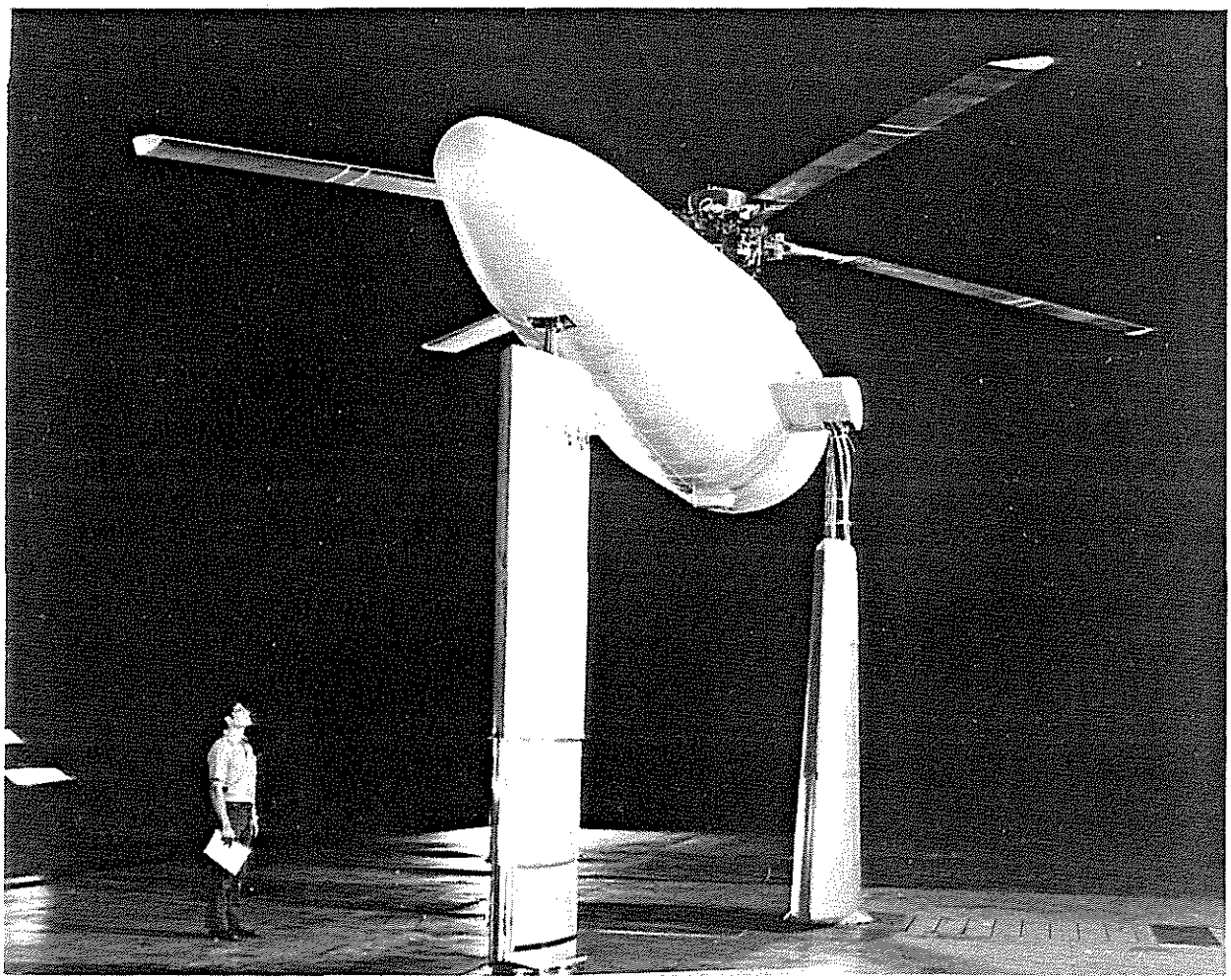

Figure 3. H-34/RTA Test Stand at NASA Ames 40 x 80 Foot Wind Tunnel

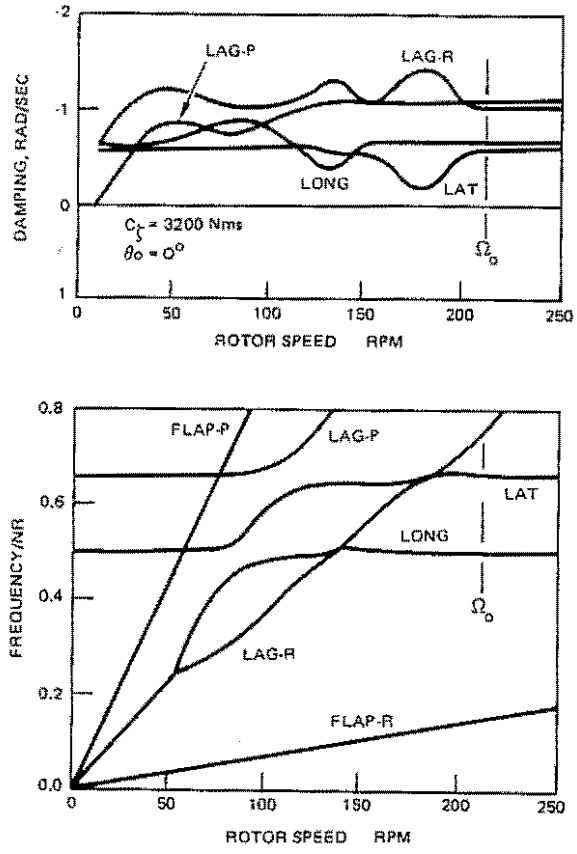

Figure 4. Modal Damping and Frequencies of H-34/RTA versus Rotor Speed at Flat Pitch and Nominal Lead-Lag Damping (Zero Controls)

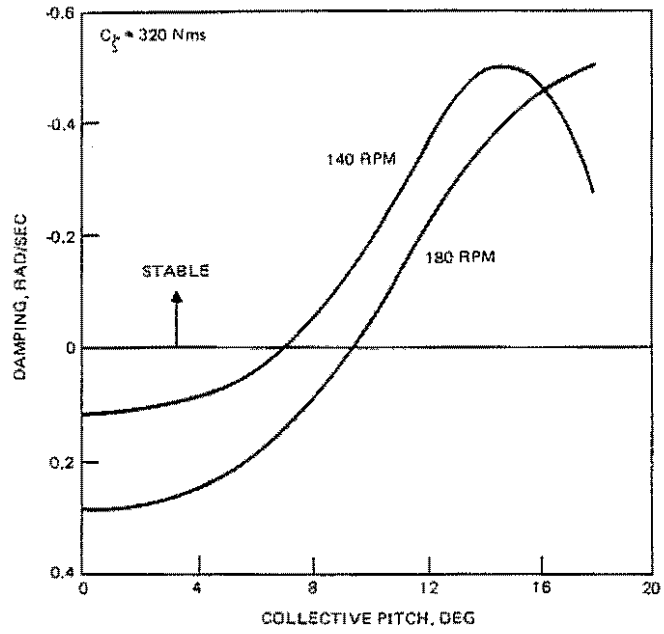

Figure 5. Effect of Collective Pitch Angle on Regressing Lag Mode Damping

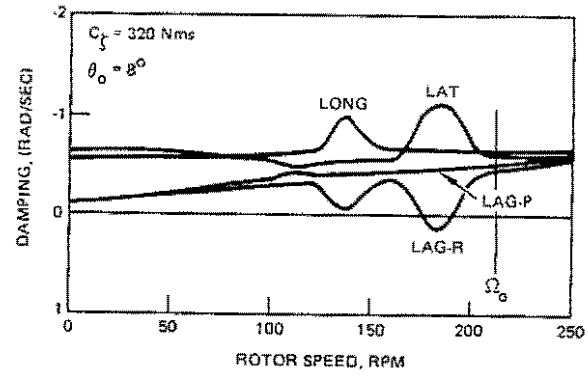

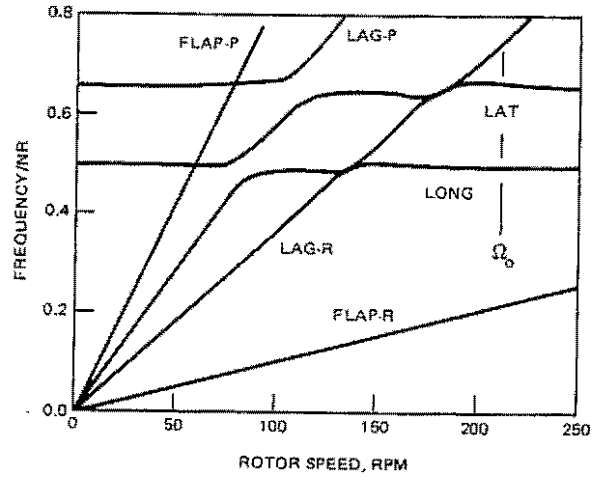

Figure 6. Modal Damping and Frequencies of H-34/RTA versus Rotor Speed at 8° Collective Pitch and Reduced Lead-Lag Damping (Zero Controls)

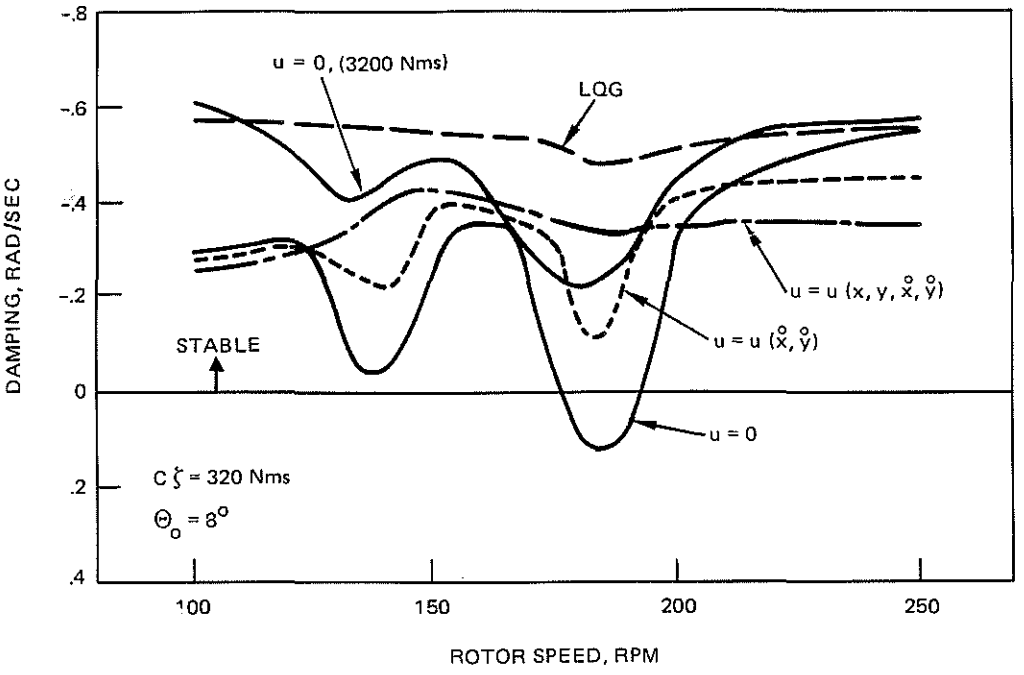

Figure 7. H-34/RTA Aeromechanical Stability With Optimal Controller and Three Reduced State, Constant Gain Feedback Systems

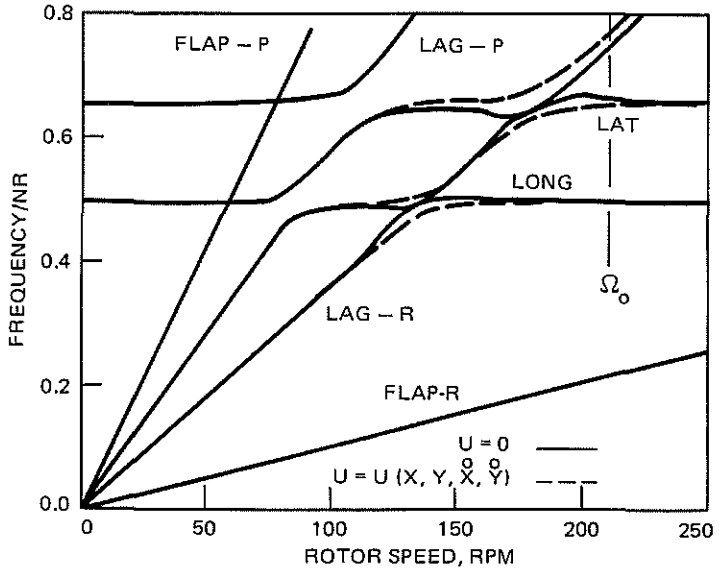

Figure 8. Effect of Feedback Control on H-34/RTA Modal Frequencies

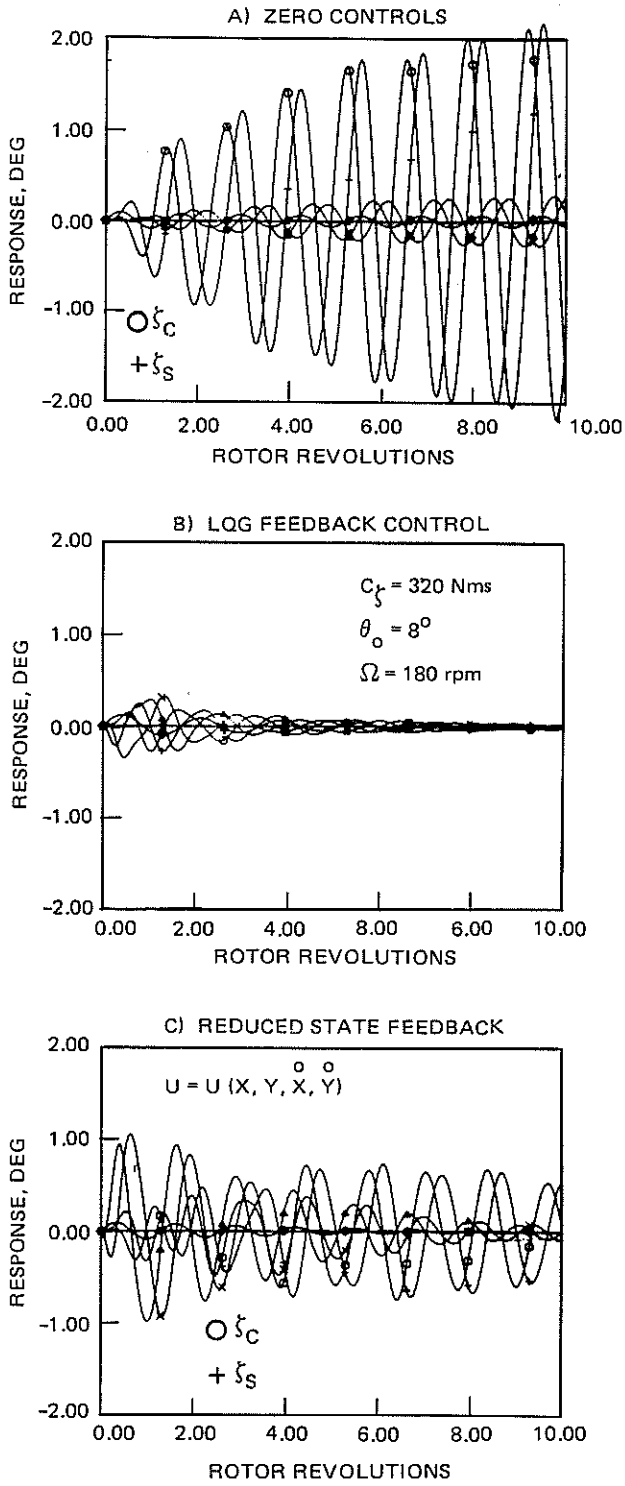

Figure 9. System Response To Lateral Rate ($\dot{R}y$) Initial Condition Showing the Effect of Active Controls (c_ζ =320 Nms, θ =8°, Ω=180 rpm)

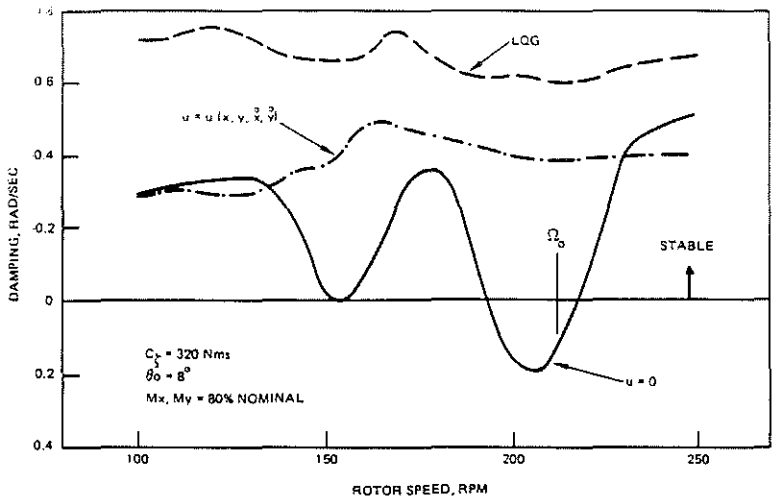

Figure 10. Controller Performance With Reduction in Support Mass Properties

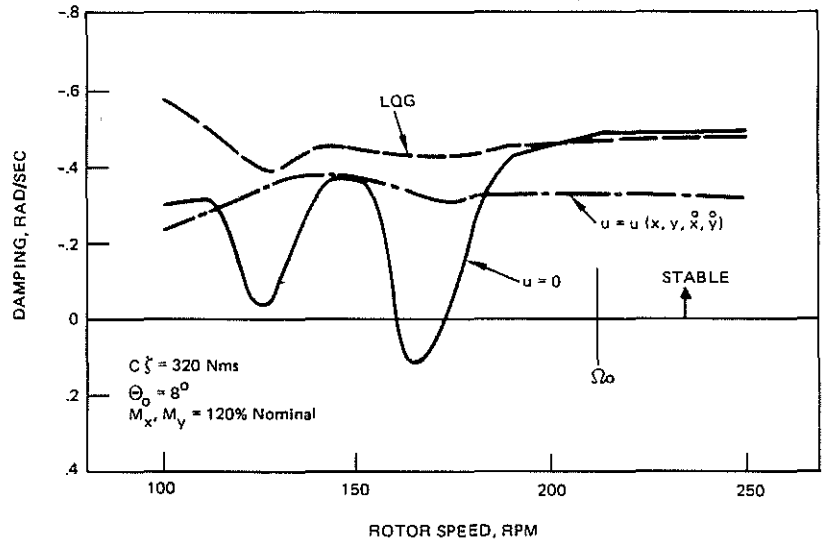

Figure 11. Controller Performance With Increase in Support Mass Properties

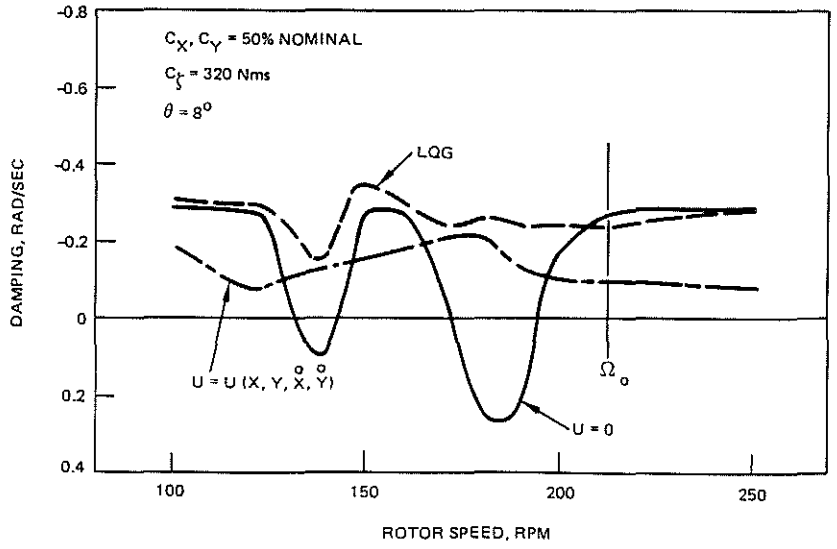

Figure 12. Controller Performance with Reduction in Support Damping Properties